Volume 6, Issue 2, 2016, 1087-1092 **ISSN 2069-5837**

Biointerface Research in Applied Chemistry

www.BiointerfaceResearch.com

Original Research Article **Open Access Journal**

Received: 03.02.2016 / Revised: 25.02.2016 / Accepted: 13.03.2016 / Published on-line: 20.03.2016

Chemical synthesis and characterization of poly (o-methoxyaniline)

Mahdi Mansour [1], Mohamed Saidi [1], Nadia Saidi-Amroun [1,*]

[1]Material Physics Laboratory, Physics Faculty, University of Sciences and Technology USTHB, BP 32 El-Alia, Bab-Ezzouar, Algiers, Algeria.

*corresponding author e-mail address:***amnadster@gmail.com**

ABSTRACT

Electrical characterizations of the silver/poly (o-methoxyaniline)/silver structure based on the charging currents and current density-voltage (*J-V*) characteristics measurements at 278 and 300 K are performed to assess its charge transport properties. The chemically prepared poly (o-methoxyaniline) (POMA) was first characterized by X-ray diffraction (XRD), UV-Vis spectrophotometry (UV-Vis), and electrical conductivity measurement. An optical band gap of 2.63 eV is evaluated from the Tauc's law and the transition is directly allowed. Further indirect transition is determined at 0.45 eV. The charging currents showed that the charge transport in POMA is considered to be a stochastic process and is bias dependent. It is found that the transport of charges is much correlated at 0.1 V than at 5 V. The lower correlation of the current at 5 V is attributed to an enhancement of charges transport. The dependences $J = f(V)$ revealed the nature of the electrical conduction mechanism. For the bias range comprises from 0.1 to 5 V, the $J = f(V)$ characteristics showed a transition from linear to a quadratic dependence at V_{tr}= 0.8 V, from which, the current increased rapidly. In order to elucidate the dominant charge transport mechanism, the $J = f(V^2)$ experimental data are found to obey to the Mott and Gurney law, and the trap free space charge limited conduction (SCLC) is taken into account.

Keywords: *poly(ortho-methoxyaniline), chemical synthesis, charging current, space charge limited current.*

1. INTRODUCTION

Since their discovery in 1977, conductive polymers were proclaimed as new futuristic materials that would lead to the generation of modern technology [1, 2]. Among them, polyaniline (PANI) and its derivatives have witnessed an impressive improvement in various potential applications including organic solar cells [3, 4], organic field effect transistors [5], lithium battery anodes [6] and chemical sensors [7] due to their advantages in terms of manufacturing cost, environmental stability, mechanical flexibility and no toxicity [8, 9]. In organic electronic devices, the interfaces with the outer contacts are believed to be one of the main factors affecting their performances. Therefore, the knowledge of the charge transfer processes at the metal/organic semiconductor interface is vital for better understanding the device characteristics.

Basically, when a metal forms intimate contact with a semiconductor, an equalization of the Fermi level of both materials occurs at thermal equilibrium. The contact metal/semiconductor may be rectifying or Ohmic depending on the type of semiconductor and the work function of the metal. The first case is known as Schottky barrier device where the limiting region of device operation is injection limited conduction (ILC) [10, 11]. In such a case, the transport properties can be analyzed in terms of the well-known classical models like Fowler-Nordheim tunneling, Poole Frenkel, or Richardson Schottky thermoionic emission [10]. Unlike classical semiconductors, heterogeneous and disordered materials like organic semiconductors cannot be treated by these mechanisms because of the backflow of the injected carriers into the electrodes which therefore makes the conduction a complex phenomenon. In contrast, if the barrier height at the metal/organic semiconductor contact is less enough, the electrode acts as charge carriers reservoir from which electrons or holes are injected into the organic semiconductor. Thus the transport properties are governed by the bulk of the material [11, 12].

Moreover, the characterization of metal/organic semiconductor/metal structure is among critical tools to estimate the basic material properties and parameters such as electrical conduction mechanism, electrical conductivity, charge carriers mobility and their concentration. According to this configuration, the active material must be embedded between two metal electrodes in which one of them should have good injection properties even at low electric field. Furthermore, the occurrence of bulk limited conduction namely bulk controlled space charge limited conduction (SCLC) requires at least that one contact forms a low potential barrier with the active material in order to provide an inexhaustible carriers reservoir.

In spite of the fact that the charge transport across the metal/semiconducting polymer interface was intensively studied in the past decades, the problem still remains under debate owing to its importance [13].

Poly (ortho-methoxyaniline) (POMA) is a PANI derivative in which a methoxy group (OCH_3) is substituted in the ortho position of the aromatic ring of the aniline monomer. In regard to POMA, one of its attractive features is to provide better solubility in common organic solvents as well as a better processability and compatibility in particular with thermoplastics compared to PANI [14]. Therefore, blends based on POMA are expected to enhance the potential applications. However, to the best of our knowledge, apart studies related to the conduction mechanisms through localized states [15, 16], there are no papers in the literature on the charges transport taking place at metal/POMA/metal structure. Therefore, POMA prepared by oxidation method was selected and

embedded between two silver (Ag) electrodes for the electrical characterization.

In the present work, we report the electrical characterization of POMA elaborated by chemical route. The obtained POMA powder was then pelletized and characterized by X-ray diffraction (XRD), UV-Vis, and electrical conductivity measurement. The charge transport nature at the metal/POMA interface is elucidated by measuring and analysing the current-voltage characteristics and charging currents variation of the Ag/POMA/Ag configuration at 278 and 300 K.

2. EXPERIMENTAL SECTION

2.1. Material preparations.

O-methxyaniline (OMA) monomer, ammonium peroxydisulfate (APS), N, N-Dimethylformamide (DMF) and p-toluene sulfuric acid (PTSA), were purchased from Sigma Aldrich and used as received. POMA was synthesized by chemical oxidative reaction of o-methoxyaniline unit (0.005 mol) in acidic solution using APS (0.005 mol) as oxidizing agent. OMA was dissolved in DMF (3 mL) and cooled at 0 °C, then the solution was mixed to p-toluene sulfuric acid (PTSA) (0.025 mol) dissolved in 50 mL of de-ionized water. The polymerization was then initiated by drop wise addition of the oxidant solution containing dissolved APS in pre-cooled de-ionized water at 0 °C under continuous magnetic stirring (2000 rpm) at ambient temperature for 5 h. The dark POMA precipitants were filtered using Whatman filter papers, washed with de-ionized water and acetone and dried in vacuum oven at 70 °C for 8 h. The obtained powder was then treated in ammonia solution (8 h) in order to get the baseform of POMA. Finally, the dried powder was cold pressed into cylindrical pellets (Ø = 13 mm, thickness = 1.8 mm) under 10 tons/cm for 2 min. The pellets exhibited a high compactness and good mechanical properties. The molecular structure of poly (o-methoxyaniline) is shown in Figure. 1.

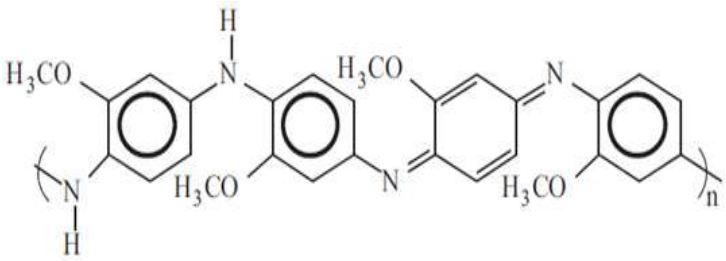

Figure 1. Chemical structure of poly (o-methoxyaniline).

2.2. Experimental part.

The room temperature conductivity of sample in the base form, measured by the standard four probe technique, is found to be 7.5 x 10^{-7} S/cm. The p type behavior of the sample is evidenced by the hot probe method.

X-ray diffraction was performed on POMA pellet by a monochromatized X-ray diffractometer using Cu-Kα radiation (λ = 1.5418 A°) operating at 40 kV and 20 mA. The 2θ range was selected from 0° to 90° with a scanning speed of 0.02 s^{-1}. The UV-visible spectrum is recorded at room temperature with a double beam spectrophotometer (Specord 200 plus), equipped with an integrating sphere; PTFE is used as reference.

A two electrodes cell assembly was used for the current-voltage curves and the current across the Ag/POMA/Ag structure measurements both at 278 and 300 K. Before these measurements, the pellet was first coated with silver paste on both sides according to gap geometry. Thereafter, the Ag/POMA/Ag system was placed between two electrodes for the electrical characterization under vacuum. The DC voltage was supplied by a stabilized HP 6206B DC power supply and the current was measured by a Keithley 617 programmable electrometer. For charging current measurements, the sample was charged for a time t_c= 2000 s followed by the discharging process for each applied voltage with the same polarization time prior to the next measurement. For the current-voltage characteristics, the measurements were performed in the polarization voltage range (0.1–5 V) using the same protocol as the previous one, except for the polarization and the depolarization time that is equal to 100 s instead of 2000 s. The isochronal currents data were extracted from these measurements in order to provide the representation of the current-voltage characteristics. The programmable electrometer is controlled by a computer via a GPIB card.

3.RESULTS SECTION

3.1. XRD analysis.

The XRD pattern (Figure. 2) does not show any sharp and well defined peaks indicating rather an amorphous sample; only a broad peak which lies between 6-30°. This broad peak is in fact typical for the amorphous nature of POMA. The main peak or maximum is situated at 25° and another weak peak near 17° is attributed to the interplanar distance of OMA-OMA rings. Indeed, it has been reported in the literature that the structure of conjugated polymers differs and depends on the polymerization type. Wolter et al [17] have predicted the XRD pattern of PANI synthesized by different routes to have amorphous to crystalline nature with different percentage.

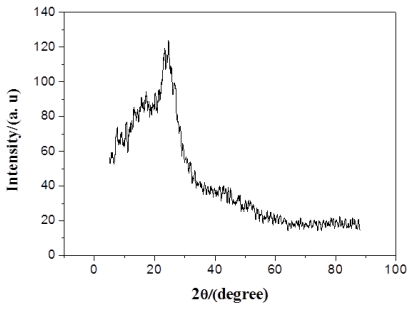

Figure 2. XRD pattern of poly (o-methoxyaniline).

3.2. UV-Visible spectroscopy.

The UV-Vis spectroscopy is used to reflect the electrical conductivity and optical absorption characters. Basically, the

energy band structure of conjugated polymers consists of the lowest unoccupied molecular orbital (LUMO) or the valence band separated by the optical gap (*Eg*) from the highest occupied molecular orbital (HOMO) or the conduction band. The UV-Vis absorption spectrum of our investigated POMA is depicted in Figure 3.

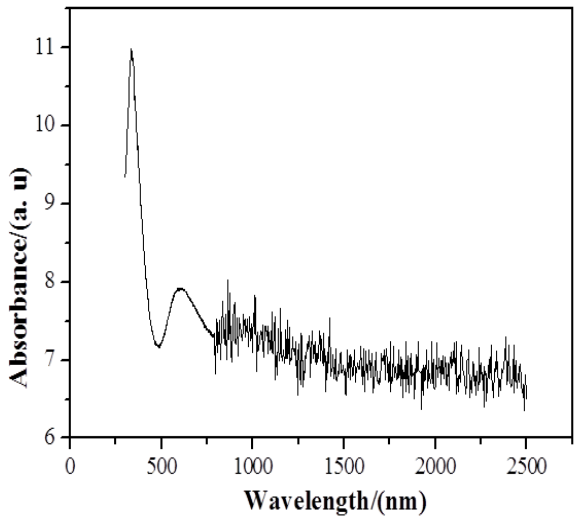

Figure 3. UV-Vis spectra of POMA.

It exhibits two major absorption bands with λ_{max} at 333 and 616 nm. The absorption band appearing at 333 nm is assigned to the π-π* electronic transition (from LUMO to HOMO) of the aromatic rings, while the band centered at 616 nm is attributed to the n- π* excitonic transition from the HOMO of the aromatic rings to the LUMO of the quinoid rings [18-20].

It is well known that the absorption coefficient α of an amorphous semiconductor has a characteristic relation expressed by Tauc [21]:

$$\alpha h\nu = A\left(h\nu - E_g\right)^n \quad (1)$$

In which $h\nu$ is the photon energy, A a constant characteristic of the material, and n an exponent that characterizes the absorption process: n = 1/2 and 2 for direct and indirect allowed transitions respectively.

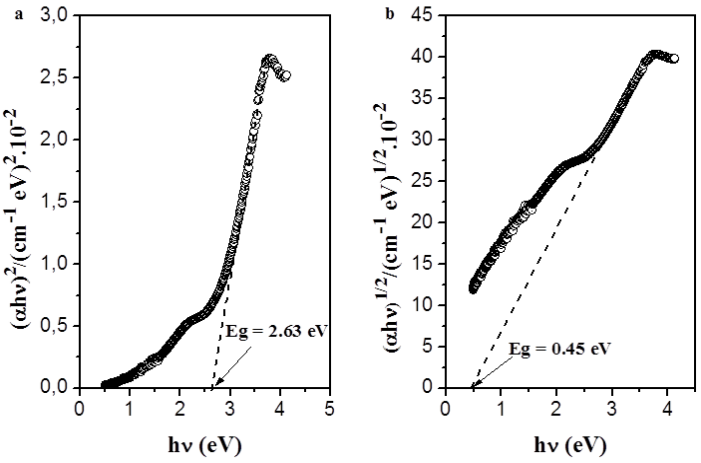

Figure 4. The direct (a) and indirect (b) optical transitions of POMA.

While taking into account these suggestions, a coexistence of direct and indirect transitions have been estimated by applying the models for both cases. For this, the $(\alpha h\nu)^2$ and $(\alpha h\nu)^{1/2}$ vs $h\nu$ respectively for direct and indirect transitions were plotted and are represented in Figure. 4.

By extrapolating the straight parts of these curves to the $h\nu$ axis, the direct and indirect band gaps were determined and found to be 2.63 and 0.45 eV respectively. Moreover, the strong linear portion of the $(\alpha h\nu)^2$ vs $h\nu$ at the absorption edge confirms that our POMA has a direct band gap.

3.3. Charge transport properties.

In this section, we review the electrical characterization of Ag/POMA/Ag system by analyzing its charging currents over time and *J-V* characteristics. Indeed, the *J-V* characteristic of such material bridging two conductive electrodes is a power tool to elucidate the charge transport nature and to determine its basic parameters. The *J-V* measurements for Ag/POMA/Ag structure at 278 and 300 K are shown in Figure. 5. To determine the current conduction mechanism in this structure, the experimental data were analyzed using the space charge limited conduction (SCLC) model. In SCLC mechanism, the conduction can be either trap free or trap filling depending upon the sample and range of applied voltage [22].

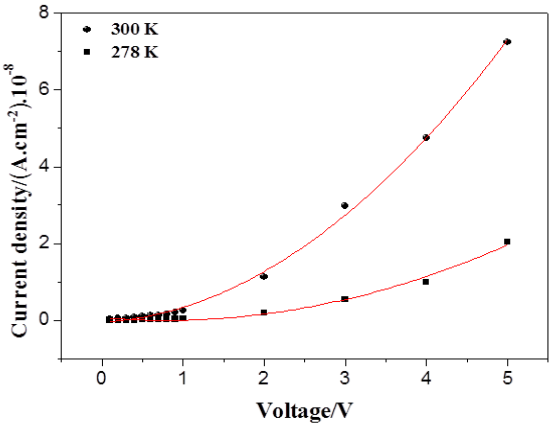

Figure 5. Current density-voltage characteristics of POMA pellet at 278 and 300 K. Solid lines represent linear fit to experimental data.

In this sense, the current density follows a power law $J \propto V^m$ where m is equal or greater than 2 for trap free or trap filling SCLC respectively. Similar behavior of current densities with applied bias is observed in our POMA sample where they show a transition from linear to a quadratic dependence over the exploited voltage range. The classical expression of the current density-voltage in that case entails a second order polynomial current density dependence on the voltage:

$$J = A + BV + CV^2 \quad (2)$$

where, A is the intercept, $B = \sigma/d$, and $C = \varepsilon_0\varepsilon_r\mu_p/d^3$. σ stands for the electrical conductivity.

By fitting the experimental data with Eq. 2, a good agreement showed the transition from a linear to quadratic current density dependence over the entire voltage range with a correlation coefficient (R^2) equal to 0.999 very close to unity, indicating that the charge transport is governed by bulk limited processes with a bias dependent crossover from Ohmic to trap free space charge limited conduction. Thus, Ag forms an Ohmic contact with POMA pellet.

Typical current density versus voltage data plotted on a logarithmic scale is shown in Figure 6. It is evident that the current

depends upon applied bias and two distinct regions have been identified at both temperatures, i.e., at lower voltage (V < 0.8 V) with a slope *m*~1 and for (V > 0.8 V) with a slope *m* ~ 2.

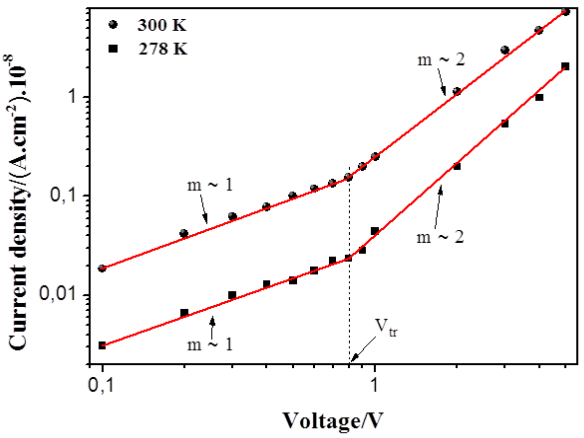

Figure 6. Log-Log representation of current density-voltage characteristics for POMA pellet. Solid lines represent linear fit to experimental data.

In the lower voltage region, the currents show Ohmic behavior originated from the thermally generated holes concentration [23, 24]. Indeed, at lower voltage, the injected carriers from the electrode do not play an important role than the intrinsic ones, and J in this case is given by the following expression:

$$J = qp_0\mu_p \frac{V}{d} \quad (3)$$

Where q is the elementary charge, p_0 for holes density generated at thermal equilibrium, μ_p the hole mobility and d the sandwiched sample thickness.

In the higher voltage region, i.e., (V > 0.8 V), the current density increases in a quadratic dependence which is characteristic of SCLC [23, 24]. SCLC occurs when the electrode supplies an unlimited number of carriers in the bulk causing a build-up of the space charge region in the sample. Furthermore, the SCLC starts to dominate the charge transport at the transition voltage (V_{tr} = 0.8 V), where the number of injected charges considerably exceeds the intrinsic charges lying in the bulk. In this regime, the current curve follows the Mott and Gurney law from which the constant mobility can be obtained. The current density dependence on applied bias is expressed by the relation [22, 25]:

$$J = \frac{9}{8}\varepsilon_0\varepsilon_r\mu_p \frac{V^2}{d^3} \quad (4)$$

Where ε_0 is the permittivity of vacuum (8.85 x 10^{-14} F cm^{-1}), and ε_r the dielectric constant.

The transition from the lower voltage region to the higher one takes places at a potential V_{tr} = 0.8 V expressed as [26]:

$$V_{tr} = \frac{8qp_0}{9\varepsilon_0\varepsilon_r} d^2 \quad (5)$$

According to Eq. 4, the dependences $J = f(V^2)$ at 278 and 300 K should give straight lines supposing that the charge mobility does not depend on the applied voltage. In Figure 7, these characteristics are illustrated for both temperatures.

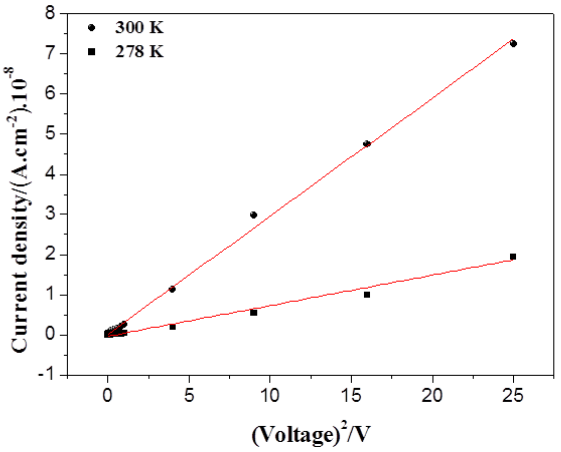

Figure7. Plot of J versus V^2 for POMA pellet at 278 and 300 K. Solid lines represent linear fit to experimental data

It can easily be observed from this Figure that the dependence $J = f(V^2)$ is linear at both temperatures and this behavior confirms that the trap free SCLC is the dominant mechanism in the studied sample. The holes concentration p_0 generated at thermal equilibrium can be determined from V_{tr} for which the transition from Ohmic to SCLC regimes takes place; the estimated value of p_0 is 3.35 x 10^{17} m^{-3} in our sample. From the slope of the fitted data with Eq. 4, hole mobilities of 1.15 x 10^{-3} cm^2 V^{-1} s^{-1} and 4.55 x 10^{-3} cm^2 V^{-1} s^{-1} at 278 and 300 K were calculated respectively. Thus, the charge carrier mobilities of our POMA report comparable values to that of electrochemically elaborated low oxidized POMA [27].

Moreover, the charges transport across the metal/semiconductor system is usually accounted for on the basis of Ohmic, SCLC, thermoionic emission, or Poole-Frenkel models [28, 29]. The last two models are found to be inapplicable for our structure, as revealed by fitting their respective laws to experimental data.

It was also observed that the *J-V* characteristics have temperature dependence. The increase of the current at 300 K is probably due to the increase of phonons scattering which assists in exciting carriers and promotes the current by the charges hopping between localized states. In this sense, it is worth noting that, the hopping transport mechanism has recently been applied to amorphous organic semiconductors [30], where two important cases are distinguished as a function of temperature. At low temperatures, the charge carriers delocalization is entirely achieved by impurities scattering [31], while at finite temperatures, the phonons scattering dominates over the impurities one and the carriers delocalization occurs as a result of phonons absorption [31-33]. In this case, the phonon assisted hopping between localized states is driven by their charge-phonon interactions. These interactions facilitate the absorption of phonons that accompany a phonon assisted hop. Thus, at 300 K the phonons assist the electrical current due to which charges hopping increases with rise in temperature, since at room temperature more phonons are available.

In Figure 8a and Figure 8b, we show the time variation of the charging electrical currents at 278 and 300 K respectively. As can be seen from these curves, short transient regimes that manifest at the beginning of the polarization (probably due to charging of interface states at Ag/POMA interface) followed by a slight increase of the current over the polarization time except for the measured current at 278 K under low bias, i.e., 0.1 V, where it shows almost a constant regime. One can attribute this last regime to an intrinsic charges limited current where the required energy for carriers delocalization is low enough. In contrast, the same measurement at 300 K does not exhibit this behavior since the charge delocalization can be achieved by thermal phonons scattering.

One can also observe in Figure 8 that, all measured currents are noisy in shape after transient regime for both applied biases and are clearly distinguishable. As Figure 8a and Figure 8b indicate, large parts of stochastic components that consist of random fluctuations of electrical currents across the sample are visible. This is probably due to the random distribution of localized states [34-36] that is a major reason for disorder, implying inhomogeneous properties, resulting in stochastic process of the electrical transport. One can also observe in Figure 8 that, all measured currents are noisy in shape after transient regime for both applied biases and are clearly distinguishable. As Figure 8a and Figure 8b indicate, large parts of stochastic components that consist of random fluctuations of electrical currents across the sample are visible. This is probably due to the random distribution of localized states [34-36] that is a major reason for disorder, implying inhomogeneous properties, resulting in stochastic process of the electrical transport.

The measured currents under 5 V at 278 and 300 K are about three orders of magnitude higher and exhibit less amplitudes of stochastic component than those measured under 0.1 V. Furthermore, not only the amplitude but also the structure of the noise is different for both temperatures (Figure 8). In this case, one should be able to attribute this enhanced behavior at 5 V to a change of the electrical conduction mechanism occurring in our studied sample.

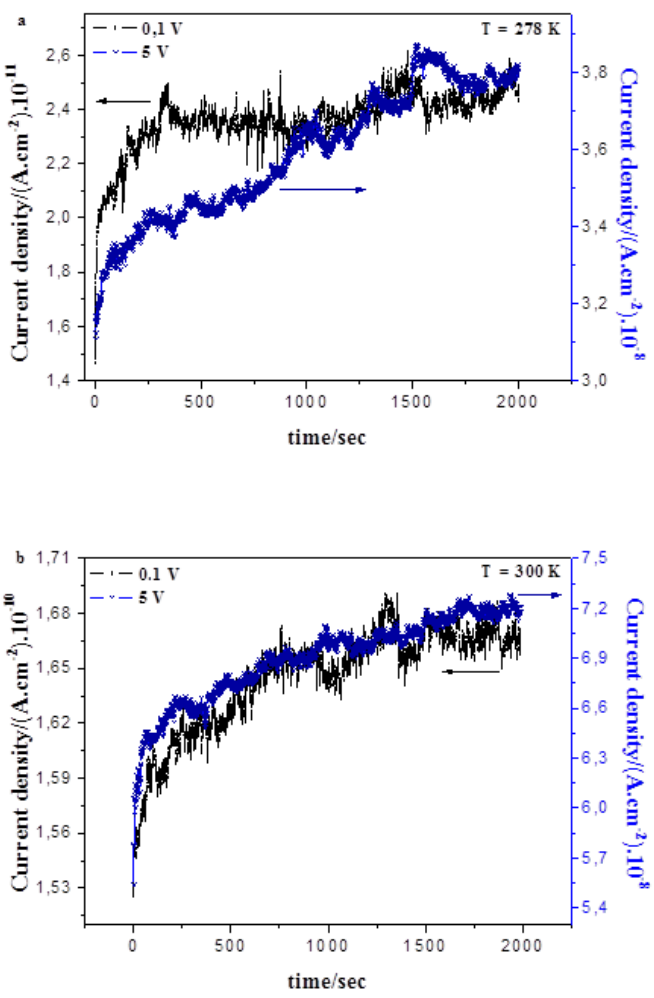

Figure 8. Charging currents (a) at 278 K and (b) at 300 K for V = 0.1 and 5 V.

Thus, it seems that at higher voltage the transport of charge carriers is less correlated than at lower voltage. This probably means that at higher voltage, the charges are likely to accumulate in the bulk leading to the formation of space charge regions near the interface that act simultaneously to ensure uncorrelated charge transport.

4. CONCLUSIONS

In summary, we have performed the electrical measurements on POMA in sandwich structure using Ag-Ag as outer electrodes. It was observed that two different regions of current dependence on bias were identified that are distinguished by a common crossover voltage (V_{tr}) at both temperatures. The SCLC is found to be the main mechanism. It starts to dominate the charge transport at the transition voltage. Until then, the charges are ohmically transported in the bulk of the sample. Thermally generated holes concentration and hole mobilities are found to be of the order of 10^{17} m^{-3} and 10^{-3} cm^2 V^{-1} s^{-1} respectively. On the other hand, the time dependence of the charging currents showed that the transport of charge carriers is considered to be as a stochastic process. It has also been observed that the correlations in the charge transport were bias dependent. At higher voltage, the charge transport is less correlated than at lower voltage. This clearly revealed that at higher voltage, the build-up of the space charge region is responsible event for the uncorrelated transport.

5. REFERENCES

[1] Nalwa H.S., *Handbook of Advanced Electronic and Photonic Materials and Devices*, 1st ed., San Diego, Academic Press, **1999.**

[2] Nalwa H.S., *Handbook of Organic Conductive Molecules and Polymers*, 1st ed., New York, John Wiley and Sons, **1997.**

[3] Onmori R.K., Olivati C.A., Bianchi R.F., Faria R.M., De Andrade A.M., Study of a POMA based solar cell, *Synthetic Metals,* 121, 1577-1578, **2001.**

[4] Onmori R.K., Dirani E.A.T., Faria R.M., De Andrade A.M., Photovoltaic effect on μc-Si :H(n+)/Poly(o-methoxyaniline)/a-Si:H(p) structures, *Synthetic Metals,* 102, 1004-1005,**1999.**

[5] Bianchi R.F., Onmori R.K., Goncalves D., De Andrade A.M., Faria R.M., Irene E.A., An electrical study of a thin film poly(o-methoxyaniline) field effect transistor, *Synthetic Metals,* 121, 1687-1688,**2001.**

[6] Wang S., Hu L., Hu Y., Jiao S., Conductive polyaniline capped Fe_2O_3 composite anode for high rate lithium ion batteries, *Materials Chemistry and Physics,* 146, 289-294,**2014.**
[7] Fratoddi I., Venditti I., Cametti C., Russo M.V., Chemiresistive polyaniline-based gas sensors: A mini review, *Sensors and Actuators B: Chemical,* 220, 534-548,**2015.**
[8] Taunk M., Kapil A., Chand S., Hopping and tunnelling transport over a wide temperature range in chemically synthesized doped and undoped polypyrrole, *Solid State Communications,* 150, 1766-1769, **2010.**
[9] Stakhira P., Cherpak V., Volynyuk D., Hotra Z., Belukh V., Aksimentyeva O., Tsizh B., Monastyrskyi L., Growth and properties of conducting polyaniline thin films obtained by means of ionic sputtering in crossed electrical and magnetic fields, *Review on Advanced Materials Science,* 23, 180-184, **2010.**
[10] Lampert M.A, Mark P., *Current Injection in Solids*, 2nd ed., New York, Academic Press, **1970.**
[11] Evgeny Y.T, Igor Z., *Handbook of Spin Transport and Magnetism*, 3rd ed., Boca Raton, Taylor and Francis Group, **2012.**
[12] Roberts G.G., Apsley N., Munn R.W., Temperature dependent electronic conduction in semiconductors, *Physics Reports,* 60, 59-150, **1980.**
[13] Hwang J., Wan A., Kahn A., Energetics of metal-organic interfaces: New experiments and assessment of the field, *Materials Science and Engineering: R: Reports,* 64, 1-31, **2009.**
[14] Hasbullah H., Kumbharkar S., Ismail A.F., Li K., Asymmetric hollow fiber membranes based on ring-substituted polyaniline and investigation towards its gas transport properties, *Journal of Membrane Science,* 397, 38-50, **2012.**
[15] Nogueira J.S., Mattoso L.H.C., Faria R.M, Ac conductivity of poly(o-methoxyaniline), *9th IEEE International Symposium on Electrets,* Shanghai, China, 145-150, **1996.**
[16] R. M. Faria, C. M. Lepiensk, J. S. Nogueira, L. H. C. Mattoso, Ac conduction of polyaniline and poly(o-methoxyaniline)*, Proceedings of IEEE Conference on Sciences and Technology of Synthetic Metals*, Seoul, Korea, 74, **1994.**
[17] Wolter A., Rannou P., Travers J.P., Gilles B., Djurado D., Model for aging in HCL-protonated polyaniline: Structure, conductivity, and composition studies, *Physical Review B,* 58, 7637-7647, **1998.**
[18] Fatuch J.C., Oviedo M.A.S., Avellaneda C.O., Franco M.F., Romao W., De Paoli M.A., Nogueira A.F., Synthesis and characterization of aniline copolymers containing carboxylic groups and their application as sensitizer and hole conductor in solar cells, *Synthetic Metals,* 159, 2348-2354, **2009.**
[19] Wang X., Ray S., Nikolaidis M.G., Easteal A.J., The effects of dopant acids on structure and properties of poly(o-methoxyaniline), *Journal of Polymer Science Part A: Polymer Chemistry,* 50, 353-361, **2012.**
[20] Sankar A., Kumaravel M., Rameshkumar S., Vijayan M., Chemical synthesis of conductive poly(methoxyaniline) in hydroxyethylidenediphosphonic acid, *Asian Journal of Chemistry,* 25, 3001-3004, **2013.**
[21] Tauc J., Menth A., States in the gap, *Journal of Non-Crystalline Solids*, 8, 569-585, **1972.**
[22] Blom P.W.M., Tanase C., de Leeuw D.M., Coehoorn R., Thickness scaling of the space charge limited current in poly(p-phenylenevinylene), *Applied Physics Letters,* 86, 092105, **2005.**
[23] Varo P.L., Tejada J.A.J., Villanueva J.A.L., Carceller J.E., Deen M.J., Modeling the transition from ohmic to space charge limited current in organic semiconductors, *Organic Electronics,* 13, 1700-1709, **2012.**
[24] Varo P.L., Tejada J.A.J., Villanueva J.A.L., Deen M.J., Space charge and injection limited current in organic diodes: A unified model, *Organic Electronics,* 15, 2526-2535, **2014.**
[25] Mott N.F., Gurney R.W., *Electronic Processes in Ionic Crystals*, 2nd ed., Oxford, Clarendon Press, **1940.**
[26] Jain S.C., Willander M., Kumar V., *Conducting organic materials and Devices*, 1st ed., Oxford, Academic Press, **2008.**
[27] Patil R., Jiang X., Harima Y., Mobilities of charge carriers in poly(o-methylaniline) and poly(o-methoxyaniline), *Electrochimica Acta,* 49, 4687-4690, **2004.**
[28] Elmansouri A., Outzourhit A., Oueriagli A., Lachkar A., Hadik N., Achour M.E., Abouelaoualim A., Berrada K., Ameziane E.L., Spectroscopic characterization of electrodeposited poly(o-toluidine) thin films and electrical properties of ITO/Poly(o-toluidine)/Aluminum Schottky diodes, *Active and Passive Electronic Components,* 2007, Article ID 17846, **2007.**
[29] Elmansouri A., Outzourhit A., Oueriagli A., Lachkar A., Hadik N., Achour M.E., Abouelaoualim A., Malaoui A., Berrada K., Ameziane E.L., Fabrication and characterization of Schottky diodes and thin films based on poly(o-toluidine) deposited by spincoating technique, *Synthetic Metals,* 160, 1487-1492, **2010.**
[30] Kapil A., Taunk M., Chand S., Preparation and Charge Transport Studies of Chemically Synthesized Polyaniline, *Journal of Materials Science: Materials in Electronics,* 21, 399-404, **2010.**
[31] Prigodin V.N., Epstein A.J., Novel mechanism of charge transport in highly doped electronic polymers, *Synthetic Metals,* 125, 43-53, **2002.**
[32] Taunk M., Kapil A., Chand S., Chemical synthesis and low temperature electrical transport in polypyrrole doped with sodium bis(2-ethylhexyl) sulfosuccinate, *Journal of Materials Science: Materials in Electronics,* 22, 136-142, **2011.**
[33] George S.D., Saravanan S., Anantharaman M.R., Venkatachalam S., Radhakrishnan P., Nampoori V.P.N., Vallabhan C.P.G., Thermal characterization of doped polyaniline and its composites with CoPc, *Physical Review B,* 69, 235201, **2004.**
[34] Fishchuk I.I., Kadashchuk A., Hoffmann S.T., Athanasopoulos S., Genoe J., Bässler H., Köhler A., Unified description for hopping transport in organic semiconductors including both energetic disorder and polaronic contributions, *Physical Review B,* 88, 125202, **2013.**
[35] Coropceanu V., Cornil J., Filho D.A.D.S., Olivier Y., Silbey R., Brédas J.L., Charge transport in organic semiconductors, *Chemical Reviews,* 107, 926-952, **2007.**
[36] Yao Y., Si W., Yang W.C., Wu C.Q., Charge transport in organic semiconductors: From incoherent to coherent, *Chinese Science Bulletin,* 58, 2669-2676, **2013.**